SPIN CHARACTERISTICS OF THE 60-mm HIGH EXPLOSIVE M49A4 PROJECTILE WITH MODIFIED M2 FIN ASSEMBLIES

Gregory Malejko

June 1996

U.S. ARMY ARMAMENT RESEARCH, DEVELOPMENT AND ENGINEERING CENTER

Armament Engineering Directorate

Picatinny Arsenal, New Jersey

US ARMY
TANK AUTOMOTIVE AND
ARMAMENTS COMMAND
ARMAMENT RDE CENTER

DTIC QUALITY INSPECTED 1

19960813 009

REPORT DOCUMENTATION PAGE

Form Approved OMB No. 0704-0188

1. AGENCY USE ONLY (Leave blank)	2. REPORT DATE June 1996	3. REPORT TYPE AND DATES COVERED

4. TITLE AND SUBTITLE

SPIN CHARACTERISTICS OF THE 60-mm HIGH EXPLOSIVE M49A4 PROJECTILE WITH MODIFIED M2 FIN ASSEMBLIES

5. FUNDING NUMBERS

6. AUTHOR(S)

Gregory Malejko

7. PERFORMING ORGANIZATION NAME(S) AND ADDRESSES(S)

ARDEC, AED
Materials and Aeroballistics Technology Division (AMSTA-AR-AET-A)
Picatinny Arsenal, NJ 07806-5000

8. PERFORMING ORGANIZATION REPORT NUMBER

9. SPONSORING/MONITORING AGENCY NAME(S) AND ADDRESS(S)

ARDEC, DOIM
Information Research Center (AMSTA-AR-IMC)
Picatinny Arsenal, NJ 07806-5000

10. SPONSORING/MONITORING AGENCY REPORT NUMBER

Technical Report
ARAED-TR-96007

11. SUPPLEMENTARY NOTES

12a. DISTRIBUTION/AVAILABILITY STATEMENT

Approved for public release; distribution is unlimited.

12b. DISTRIBUTION CODE

13. ABSTRACT (Maximum 200 words)

The 60-mm M49A4 mortar projectile experienced large range standard deviations, short round, and excessive duds during lot acceptance tests conducted during 1992. Previous wind tunnel testing and trajectory analysis identified resonance instability as a possible cause of the poor test results. The current wind tunnel test was performed to study the spin characteristics of the M49A4 projectile with both standard and modified M2 fin assemblies. Tests performed using standard fin assemblies show the projectile develops spin rates close to the natural pitching frequency, supporting the resonance instability theory. Wind tunnel tests performed with modified fin assemblies indicate it is possible to produce enough roll torque to rapidly spin the projectile through the maintain a spin rate above the projectile's natural pitching frequency. Test firings conducted with the modified fin assemblies resulted in improved performance.

14. SUBJECT TERMS

Aerodynamics   Spin   Resonance   Subsonic   Wind tunnel   M49A4   M2 fin

15. NUMBER OF PAGES
39

16. PRICE CODE

17. SECURITY CLASSIFICATION OF REPORT UNCLASSIFIED	18. SECURITY CLASSIFICATION OF THIS PAGE UNCLASSIFIED	19. SECURITY CLASSIFICATION OF ABSTRACT UNCLASSIFIED	20. LIMITATION OF ABSTRACT SAR

NSN 7540-01 280-5500

Standard Form 298 (Rev. 2-89)
Prescribed by ANSI Std. Z39-18
298-102

CONTENTS

FIGURES

FIGURES (cont)

TABLES

ii

INTRODUCTION

The 60-mm M49A4 is a high explosive (HE) mortar projectile produced by the U.S. Army for use by the U.S. Marine Corps. After each lot of projectiles is produced, lot acceptance tests (LAT) are performed on a random sample of projectiles to ensure adequate performance. During LAT performed on the subject projectile in 1992, some production lots experienced large range standard deviations, short rounds, and excessive duds. Smear photographs taken shortly after exit from the mortar tube clearly showed the fuze windshield separated from some projectiles. To find the effect on projectile aerodynamics of the fuze windshield separation, a wind tunnel test was performed. The wind tunnel test and subsequent trajectory analysis (ref 1) showed that projectiles whose fuze windshield separates early in the flight will fall short of the intended range. The range losses observed during the LATs, however, were much larger than those that result from the fuze windshield separation. Reference 1 suggests the short rounds (as well as the other performance deficiencies) may have been due to resonance instability, caused by the projectiles spinning near their natural pitching frequency. The concern of resonance instability occurring was also raised previously in a study performed on the M49A4E2 projectile (ref 2). The goal of the current effort was to determine if it is possible to spin the projectile above the resonant frequency, by bending the rear portion of the fin blades on the M2 fin assembly.

DISCUSSION

General

The M49A4 projectile (fig. 1) is a statically stabilized, non-spinning mortar projectile. Static stability is achieved through the use of eight tail fins, mounted on the aft end of the projectile. The projectile is launched from a smooth bore weapon and the tail fins are designed to produce no roll torque, so the M49A4 projectile should not spin while in flight. Factors such as manufacturing tolerances and fin damage, however, may cause projectiles to spin. The M49A4 projectile has a low natural pitching frequency (between 0.8 and 3.8 Hz), so any roll producing asymmetry may spin the projectile near the pitching frequency. For a statically stabilized projectile, the natural pitching frequency is given by

$$f_n = \sqrt{\frac{qSdC_{m_\alpha}}{I_y}}$$

(1)

Projectiles whose spinning and pitching frequencies remain close for any substantial length of time during flight are susceptible to a resonance instability, which causes the amplitude of any trim angle to grow with time. Projectiles which undergo resonance instability may experience large range losses due to flying at increased angles of

1

attack. To minimize the possibility of resonance instability occurring, statically stabilized projectiles are typically designed to have an equilibrium spin frequency above the resonant frequency. In addition, if launched from smooth bore weapons, they should have a roll torque which is capable of rapidly spinning the projectile through the resonant frequency to avoid roll lock-in (ref 3). Resonance instability was considered a likely cause of the short rounds observed during the M49A4 LAT, so an effort was undertaken to resolve this problem. The preferred solution was to modify the fins to generate a sufficient roll torque to spin the projectile above the resonant frequency. This is normally accomplished by beveling or canting the fin blades. A decision was made to cant the aft end of the fin blades, since it was felt that this would be the most practical method to modify the large inventory of existing M49A4 projectiles.

The bore-riding surfaces near the aft ends of the fin blades (fig. 2) are critical to the projectile's travel in the mortar tube, so it was imperative that they not be altered when the fins were modified. Therefore, the proposed fin cant was to make use of the portion of fin blade aft of the bore-riding surface (approximately 1/10 in.). Due the short length of fin that was canted, the modified portion of the fin blades exhibited more of a "bend" than a "cant". Typical fin blades whose aft end are canted exhibit a distinct bend line from the fin root to the fin tip, aft of which the remainder of the fin blade is at a constant angle relative to the forward part of the fin blade. Comparison of a fin blade used in the current test with a conventionally canted fin blade is shown in figure 3. The bend angles were not constant due to the rounded shape, so the fin bend angles referred to in this report are the angles measured near the fin trailing edge. Photographs of a modified M2 fin assembly are shown in figure 4.

Wind Tunnel Test Apparatus

Facility

The wind tunnel test was conducted in the U.S. Army Armament Research, Development and Engineering Center's 24-in. subsonic wind tunnel (ref 4) between 14 June and 06 July 1993. This facility is an intermittent induction type tunnel, capable of Mach numbers from 0.30 to 0.77. Air is injected downstream of the test section, thereby inducing air to flow through the test section (fig. 5). Obtaining a desired Mach number in the test section is achieved by placing a symmetrical aluminum nozzle 12 in. downstream from the test section, thereby creating the critical area ratio necessary at the specific operating pressure to produce Mach 1.0 flow at the nozzle throat. By keeping a particular nozzle in the tunnel, the same Mach number can be repeated run after run. The tunnel test section is 36 in. long and 24 in. in diameter, and the walls are slightly divergent at an angle of 10 minutes to allow for boundary layer growth.

Models

The wind tunnel model body and boom were full scale replicas of the actual round, fabricated of aluminum. A standard M935 fuze, modified internally to render it inert, was used throughout the test. The test was conducted using standard M2 fin assemblies, which were internally modified to accommodate the wind tunnel support apparatus and whose aft ends were bent as described previously. The five configurations which were tested differed only in fin bend angle. Fin bend angles of 0, 5, 11, 18, and 45 deg were tested (a fin assembly whose fins were bent at 30 deg was also available, but never tested). The configuration numbers in this report refer to the fin bend angle. For example, configuration 11 refers to the wind tunnel model whose fins were bent to 11 deg.

The wind tunnel model was attached to a sting by means of a spin fixture, which contains two sets of ball bearings. The outer races of the ball bearings were attached to the outer body of the spin fixture, which was then fastened to the wind tunnel model. The inner races were attached to the inner body of the spin fixture, which was affixed to the sting. This setup enables the model to rotate freely about its longitudinal axis. The end of the sting opposite the model was mounted on the wind tunnel's angle of attack blade. A photograph of the wind tunnel model, mounted on the sting in the wind tunnel test section, is shown in figure 6.

The initial spin acceleration of the model was measured with the aid of a spin lock. The spin lock consisted of a thin metal rod which was placed between two fin blades and a remotely operated actuator, located on the wind tunnel's angle of attack blade, capable of pulling the rod rearward away from the fins. The spin lock restrained the model from spinning until the flow in the tunnel reached steady state (several seconds), at which time the recording equipment was turned on and the spin lock was disengaged.

Instrumentation

The projectile spin was measured using a magneto, which consisted of two magnets fixed to the model body and a coil of wire located in the spin fixture's inner body. As the model rotated such that the magnet passed over the coil, an electric current was induced and the resultant signal was recorded on a Honeywell visicorder. The visicorder uses a xenon lamp to record the data on light sensitive paper. A sample visicorder output is shown figure 7.

Test Procedure

General

The wind tunnel model to be tested and the spin fixture were mounted on the sting and attached to the angle-of-attack mechanism. Before each run, the model was positioned at the desired angle of attack and the spin lock was engaged. The tunnel was started, and after allowing several seconds for the flow to reach steady state, the spin lock was disengaged and the model was free to spin. Data was acquired from just prior to the release of the spin lock and continued until the spin rate reached steady state. This procedure was repeated until data was obtained at all the desired angles of attack. Then, either the nozzle would be changed to obtain a new Mach number or a new model was installed in the tunnel.

The bearing friction was determined by despinning the model (without the fins, to minimize the aerodynamic spin damping) while the tunnel was not operating. The model was spun up by applying a jet of high pressure air onto the model body. When the model reached the desired spin rate, the air jet was removed and the visicorder was turned on to record the spin history. The spin-down runs were performed periodically throughout the test, to ensure that no change in the bearing friction occurred.

Test Conditions

The test plans called for runs to be made at Mach numbers of 0.30 and 0.48. Mach 0.30 is the lowest that can be obtained using the available nozzles, and 0.48 is the approximate launch Mach number at charge 4. The nominal test conditions are listed in table 1. Rather than testing every configuration at many angles of attack, a decision was made to run each configuration at only zero aero angle of attack. If a particular design exhibited the desirable roll characteristics, it would then be tested over a full range of angles of attack.

Data Reduction

As mentioned earlier, the spin data was recorded on visicorder paper. Also recorded on the paper was a reference signal whose frequency was a constant 60 Hz (fig. 7). By comparing the signal produced by the spinning wind tunnel model to that of the reference signal, it was possible to determine the projectile spin rate as a function of time (keeping in mind the spin fixture contained two magnets, so the signal produced by the projectile was actually twice the model spin frequency). The model spin rate was obtained by counting the number of revolutions made by the model in a given time period, and then dividing by that time.

4

The bearing friction was obtained from the spin-down runs by assuming that the bearing friction was the only force acting to despin the model. In reality, an aerodynamic roll damping moment also acts to despin the model. Since the fins were removed from the model for the spin down runs, this effect is relatively small and was therefore ignored. The spin rate versus time data was then fit and the bearing friction was obtained.

The spin rate versus time for the actual test runs was obtained by analyzing the visicorder traces over small time intervals. The spin rate obtained was considered the average over the time interval and was applied at the midpoint of the time interval. A sample spin rate versus time plot, obtained using this technique is shown in figure 8. Once the spin rate was established for an entire run, it was possible to obtain the aerodynamic coefficients for that particular run. The torques acting about the longitudinal axis of the model in the wind tunnel are given by

$$\Sigma\, T = T_{Roll\ Torque} + T_{Roll\ Damping} + T_{BF} = I_x \dot{p} \tag{2}$$

Or, in terms of the aerodynamic coefficients

$$C_{l_o} qSd + C_{l_p} qSd \left(\frac{pd}{2V}\right) + T_{BF} = I_x \dot{p} \tag{3}$$

At time equals zero (i.e., the instant the spin lock is removed), the model is not spinning (p=0) and the zero spin roll torque can be determined from the slope of the spin rate versus time data as follows

$$C_{l_o} = \frac{I_x \dot{p}_O - T_{BF}}{qSd} \tag{4}$$

Once the zero spin roll torque is known, the roll damping moment coefficient can be determined using the steady state spin rate measured in the tunnel. Rearranging equation 3, and solving for the spin damping moment coefficient

$$C_{l_p} = -\left(C_{l_o} + \frac{T_{BF}}{qSd}\right)\left(\frac{2V}{P_{ss}d}\right) \tag{5}$$

RESULTS

Wind Tunnel

The first model tested was configuration 45, at the Mach 0.48 test condition (zero angle of attack). This configuration had a steady state spin rate of 160 Hz in the wind tunnel, which was much higher than desired. Since it was believed that the 30 deg

5

bent fin would also produce too large of a roll torque, a decision was made not to test configuration 30. Configurations 5, 11, and 18 were all tested at both Mach 0.30 and Mach 0.48 at zero angle of attack. Table 2 lists the steady state spin rates and initial spin accelerations measured in the wind tunnel.

The aerodynamic roll coefficients were calculated from the wind tunnel data using equations 4 and 5, and are presented in table 3 (note that no coefficients are given for configuration 5, for which no initial spin acceleration was measured). The roll moment coefficients, as expected, increased with increasing fin bend angle. The roll damping moment coefficients varied from -0.29 to -0.36, and the average value of -0.33 agrees well with previously published data for a similarly shaped projectile (ref 5). The roll damping moment coefficients should be the same for all configurations tested at zero angle of attack, since they used the same body and have virtually identical fin planforms (spin damping for finned projectiles is dominated by the fin planform). Therefore, all subsequent calculations were performed using a roll damping moment coefficient of -0.3. To directly compare the roll characteristics of the different tails, the roll moment coefficients were recalculated for each configuration, using the roll damping moment coefficient of -0.3. The results are presented in table 4.

Fixing the roll damping moment coefficient to a single value enabled the roll moment coefficient to be calculated without measuring the initial spin acceleration. This is accomplished by rearranging equation 5 to solve for the roll moment coefficient. Only the steady state spin rate was measured for all wind tunnel runs performed after the decision to fix the roll damping moment coefficient.

To determine if the standard (uncanted) M2 tail assemblies were indeed imparting roll moments to the projectiles, 10 were modified for testing in the wind tunnel. One tail assembly did not align properly with the boom, so only nine of the tails were tested. Of the nine tested, only three of the tail assemblies produced enough roll torque to overcome the static bearing friction and spin the model at Mach 0.30. At Mach 0.48, every tail assembly developed enough roll torque to spin the model, with the average spin rate being 1.6 Hz. The steady state spin rates measured in the wind tunnel, and the corresponding roll moment coefficients are presented in table 5. For those tails which spun the model at Mach 0.30, calculations indicate the roll torques produced by the tails were not much larger than the measured bearing friction. These results, therefore, are subject to a large error and were not used in subsequent analyses. Instead, only the coefficients obtained at Mach 0.48 were used, and assumed to be constant at lower Mach numbers.

There was concern as to the repeatability of the fin bending process, so the fin blades on 10 additional tail assemblies were bent using the same procedure that produced the first tail with the 11 deg bent fins. The original 11 deg bent fin assembly was designated configuration 11-0, and the additional 10 tails were designated configurations 11-1 through 11-10. Each of these tail assemblies were then placed on

6

the wind tunnel model and the steady state spin rate was measured at Mach numbers of 0.30 and 0.48. The steady state spin rates measured during these runs and the roll moment coefficients calculated from these data are presented in table 6. The steady state spin rates measured in the wind tunnel are plotted versus fin bend angle in figure 9. With the limited data obtained from this test (and the large spin rate variation observed for the 11 deg bent fins) it is not possible to obtain an accurate correlation between spin rate and fin bend angle.

Trajectory Simulations

The effect the various fin bend angles have on the spin of the M49A4 projectile in free flight was determined using a six degrees-of-freedom (DOF) trajectory simulation program (ref 6). All trajectories were simulated under standard atmospheric conditions (1959 ARDC standard atmospheric model) using the aerodynamic roll coefficients from tables 4 and 5 and all other aerodynamic coefficients from reference 1. The projectile mass and inertial properties used in the trajectory simulations are given in table 7. The spin histories were obtained from the six DOF trajectory simulation program and were plotted as a function of flight time.

The calculated spin histories for the M49A4 projectile with standard M2 fin assemblies, launched at a quadrant elevation (QE) of 45 deg, are plotted versus time of flight in figures 10 and 11 for charges 0 and 4, respectively. The dashed line on these plots represents the resonant pitching frequency of the projectile. As is evident from these plots, the projectiles with uncanted fins spin dangerously close to the resonant pitching frequency for a majority of their flight. Thus, the M49A4 projectile is indeed susceptible to resonance instability, which may have caused the poor range performance observed during the LAT.

Spin histories for the M49A4 projectile with various fin bend angles are presented in figure 12, for projectiles launched at charge 4 and a QE of 45 deg. Also shown in this figure is the resonant frequency, depicted by the dashed line. Configurations 11-0, 18, and 45 spun up rapidly through the resonant frequency and remained well above it for the remainder of the flight. Configuration 5 does spin up through resonance, however, it spends the majority of its flight time relatively close to the resonance frequency, which is undesirable. The fins bent to the largest angles caused very high spin rates, which should be avoided since they make the projectile susceptible to Magnus instability. When fired at charge 4, configurations 11-0 and 18 maintain spin rates high enough to avoid a resonance instability yet low enough to minimize the possibility of Magnus instability occurring.

This analysis was repeated for projectiles launched at charge 0 and a QE of 45 deg. The spin histories for the various configurations are presented in figure 13. The resonant frequency is also included in this figure for comparison. As was the case at charge 4, configuration 5 is the only design which does not spin sufficiently high to avoid the possibility of resonance instability.

7

The free flight spin histories were also calculated for configurations 11-1 through 11-10. The results are presented in figures 14 and 15, for charge 0 and 4, respectively (note there are less than 11 lines on the plots since several tails yielded the same roll coefficients, and thus produced the same spin histories). There was a large variation in spin rates (greater than 50% variation in final spin rate), although all the tails spun the projectile rapidly through and then maintained a spin rate above the resonant frequency.

Based on the results obtained using the wind tunnel test data and trajectory simulation program, a minimum nominal fin bend angle of 11 deg is desired. Due to the large variability in spin rates observed (for fins which were nominally bent to the same angle), projectiles whose nominal fin bend angles are less than 11 deg may have undesirable spin characteristics.

Supplemental Wind Tunnel Testing

Additional wind tunnel testing was performed on configuration 11-0 to determine the aerodynamic roll coefficients when the projectile is at angle of attack. All angle of attack testing was limited to one Mach number (Mach 0.30), since the previous analyses indicate no Mach number dependance (tables 4 and 7). The steady state spin rates and initial spin accelerations measured in the wind tunnel at Mach 0.30 are listed in table 8. The projectile's angle of attack had a minimal effect on the steady state spin rate. Except for the highest angles tested (20 deg), the steady state spin rates varied less than 10% from the zero angle-of-attack value. The aerodynamic roll coefficients were calculated from the wind tunnel data using equations 4 and 5 and are presented in table 9.

The aerodynamic roll coefficients at angle of attack were incorporated into the six DOF model, and additional trajectories were simulated. Large angular disturbances were introduced to the projectile at launch, causing it to fly with relatively large angles of attack for a significant portion of its flight. The results indicate the projectiles angle of attack motion has virtually no effect on its spin history.

Test Firings

To verify that bending the fins does indeed improve the flight performance of the M49A4 projectile, a series of test firings were conducted using tail assemblies whose fins were bent as previously described. Due to the large variability in fin bend angles which were seen on the fin blades modified for the wind tunnel tests, a decision was made to set the nominal bend angle at 15 deg, with a tolerance of ±4 deg. This requires all fin blades to be bent at an angle greater than 11 deg, the minimum desired based on the wind tunnel tests.

The test firings were conducted during late 1993 at Hawthorne Army Ammunition Plant, Nevada. Groups of 40 modified and 40 unmodified projectiles were tested at charges 0 and 4 at a QE of 800 mils. Test firing results indicate the modified fins improve the performance of the M49A4 projectile. The fin modifications prevented any projectiles from falling well short of the intended range, reduced the number of duds, and improved the range probable error of the groups fired (ref 7). These results indicate the unmodified projectiles were indeed being affected by a dynamic flight instability, which was eliminated with the fin modifications described in this report.

CONCLUSIONS

The 60-mm M49A4 projectile experienced large range standard deviations and excessive duds during lot acceptance tests performed during 1992.

Previous studies indicate the M49A4 projectile is susceptible to resonance instability due to its nonspinning design and low natural pitching frequency (refs 1 and 2).

A wind tunnel test was performed in the U.S. Army Armament Research, Development and Engineering Center's 24-in. subsonic wind tunnel to characterize the spin of the M49A4 projectile. Results indicate the projectile develops sufficient roll torque (due to asymmetries on the M2 tail assembly) to spin the projectile at frequencies near the natural pitching frequency.

Wind tunnel test and trajectory simulation results indicate a simple modification to the fins (bending the aft end of the blades) on the M2 tail assembly can be made to achieve desirable spin characteristics.

With the aft end of the fin blades bent to angles at or above 11 deg, enough roll torque is produced to spin the projectile rapidly up through and maintain a spin rate well above the resonant frequency.

Due to the large roll torque variability from one tail to the next, the nominal fin bend angle should be large enough to ensure no fins will have bend angles less than 11 deg.

Test firings conducted with projectiles using both modified (fin aft ends bent to 15 ±4 deg) and unmodified tail assemblies indicate the modified tail eliminated the short rounds, improved the range probable error, and reduced the number of duds. This improved performance is attributed to the improved spin characteristics of the modified projectiles.
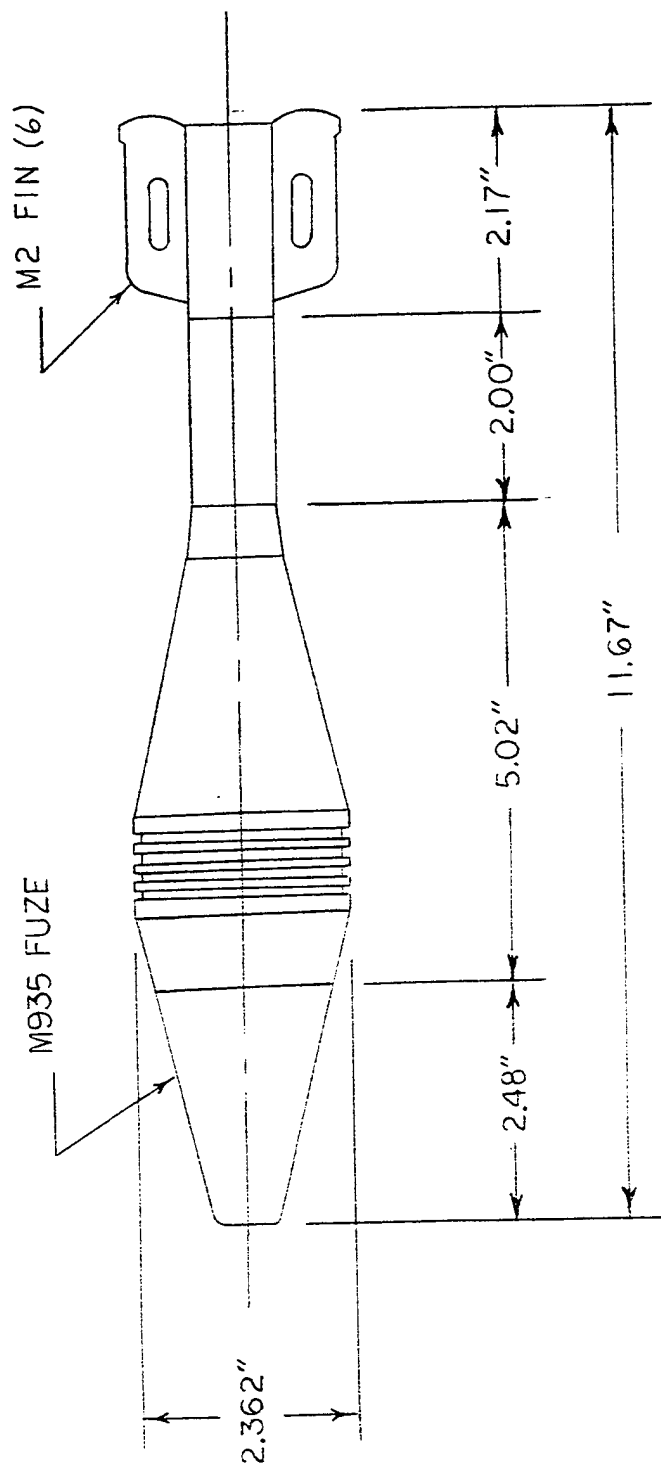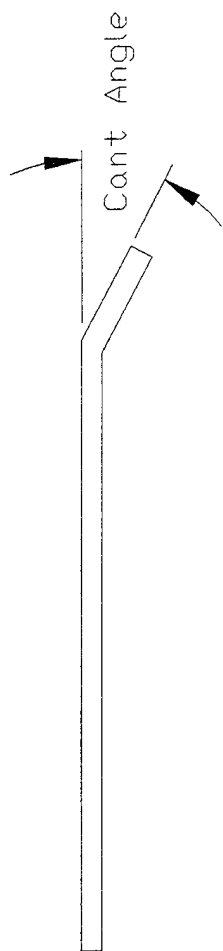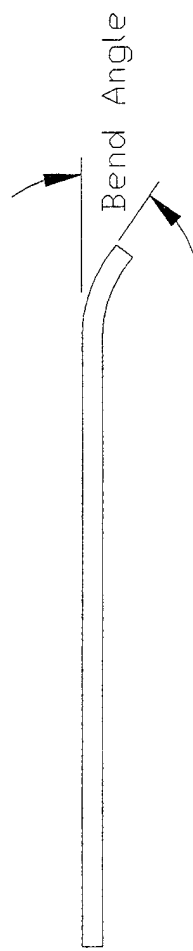
M2 FIN (6)

M935 FUZE

2.362"

2.17"

2.00"

11.67"

5.02"

2.48"

Figure 1
60-mm M49A4 mortar projectile

11

Figure 2
M2 fin assembly

12

Cant Angle

Conventionally Canted Fin

Bend Angle

Bent Fin Used in Current Study

Figure 3

Comparison of conventionally canted fin to bent fin used in current study
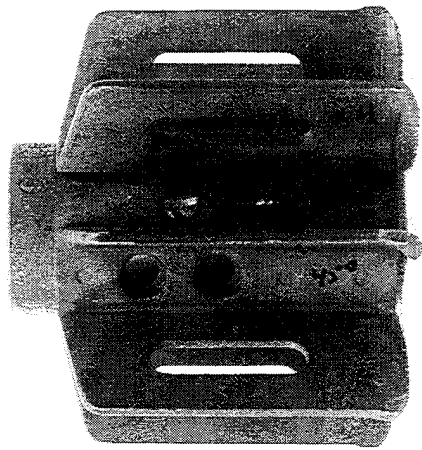
13

Figure 4
Modified M2 fin assembly

Figure 5
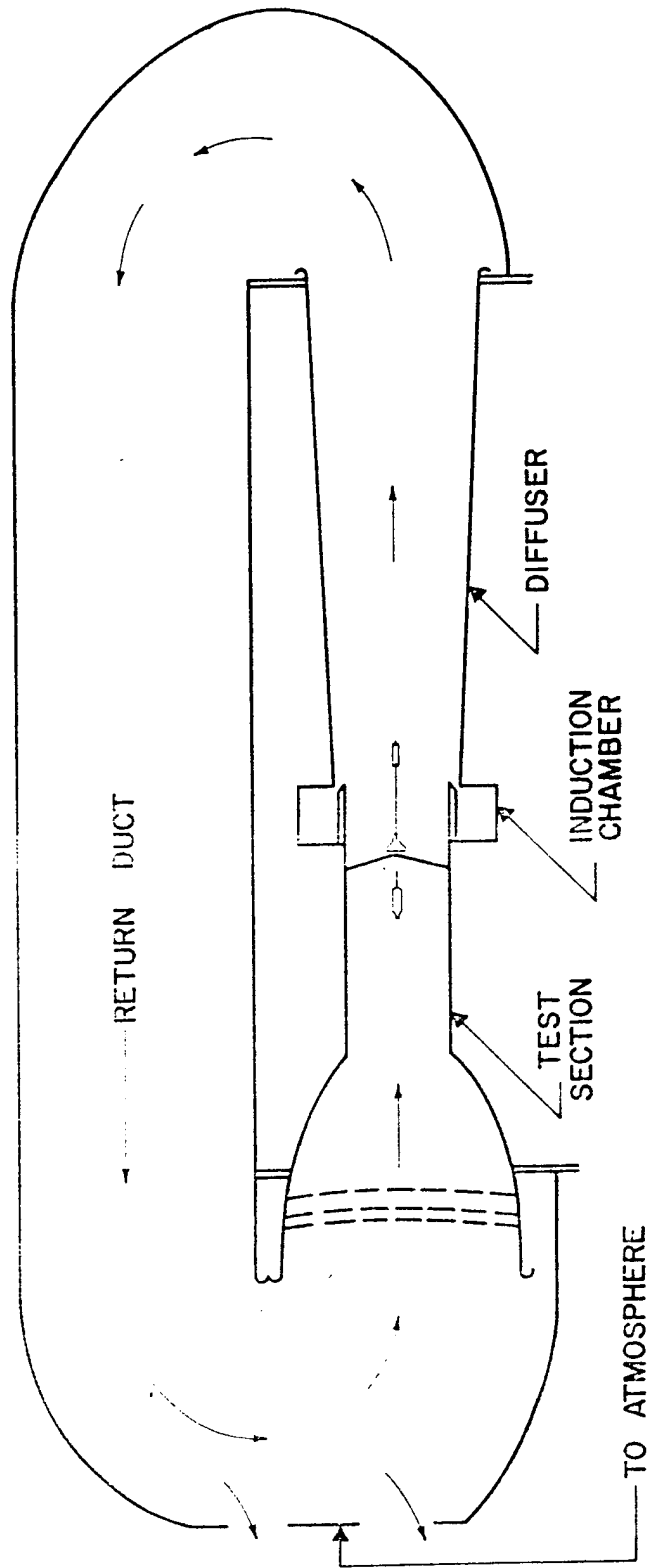ARDEC 24-in. subsonic wind tunnel
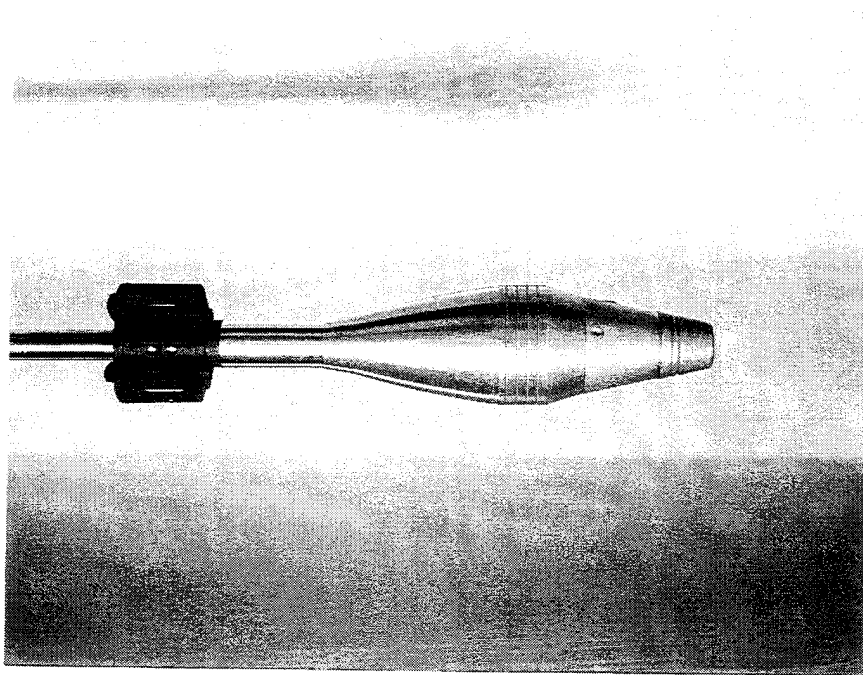
Figure 6
Wind tunnel model mounted in the wind tunnel test section

60 Hz reference signal

Signal produced by spinning model
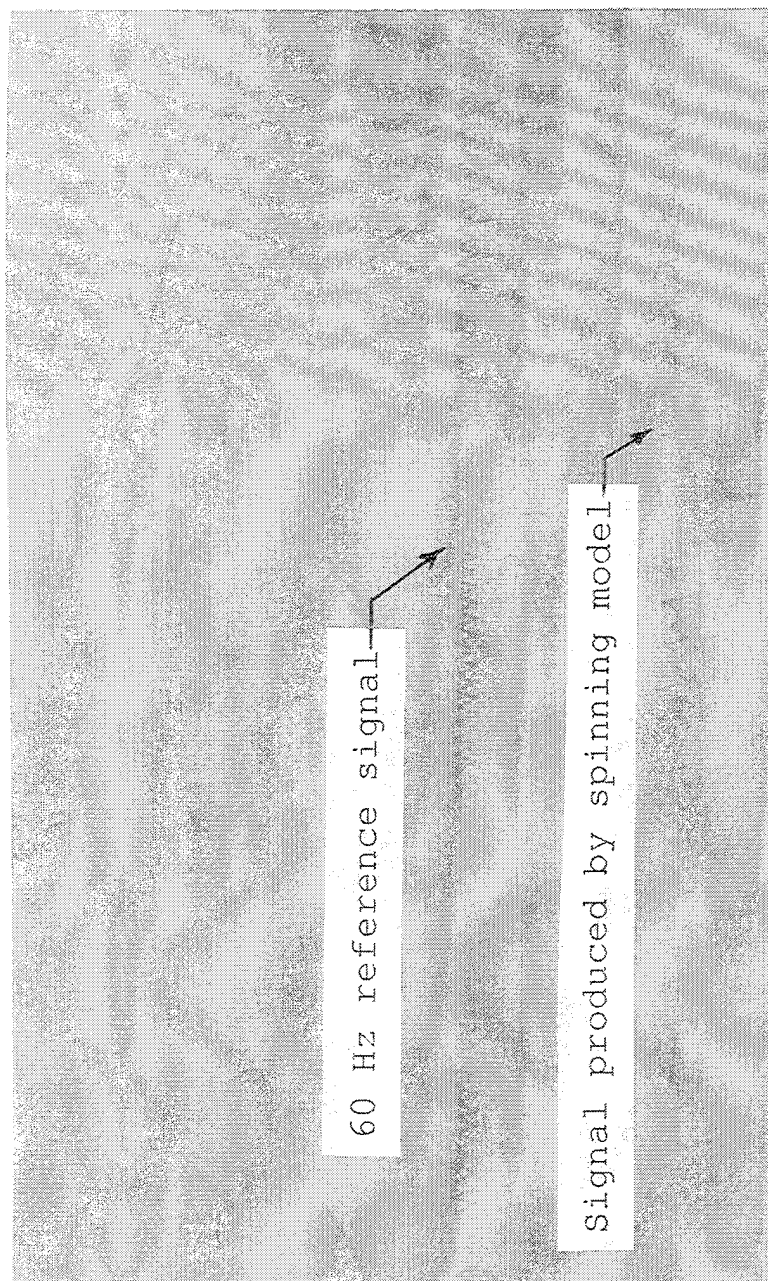
Figure 7
Sample visicorder output
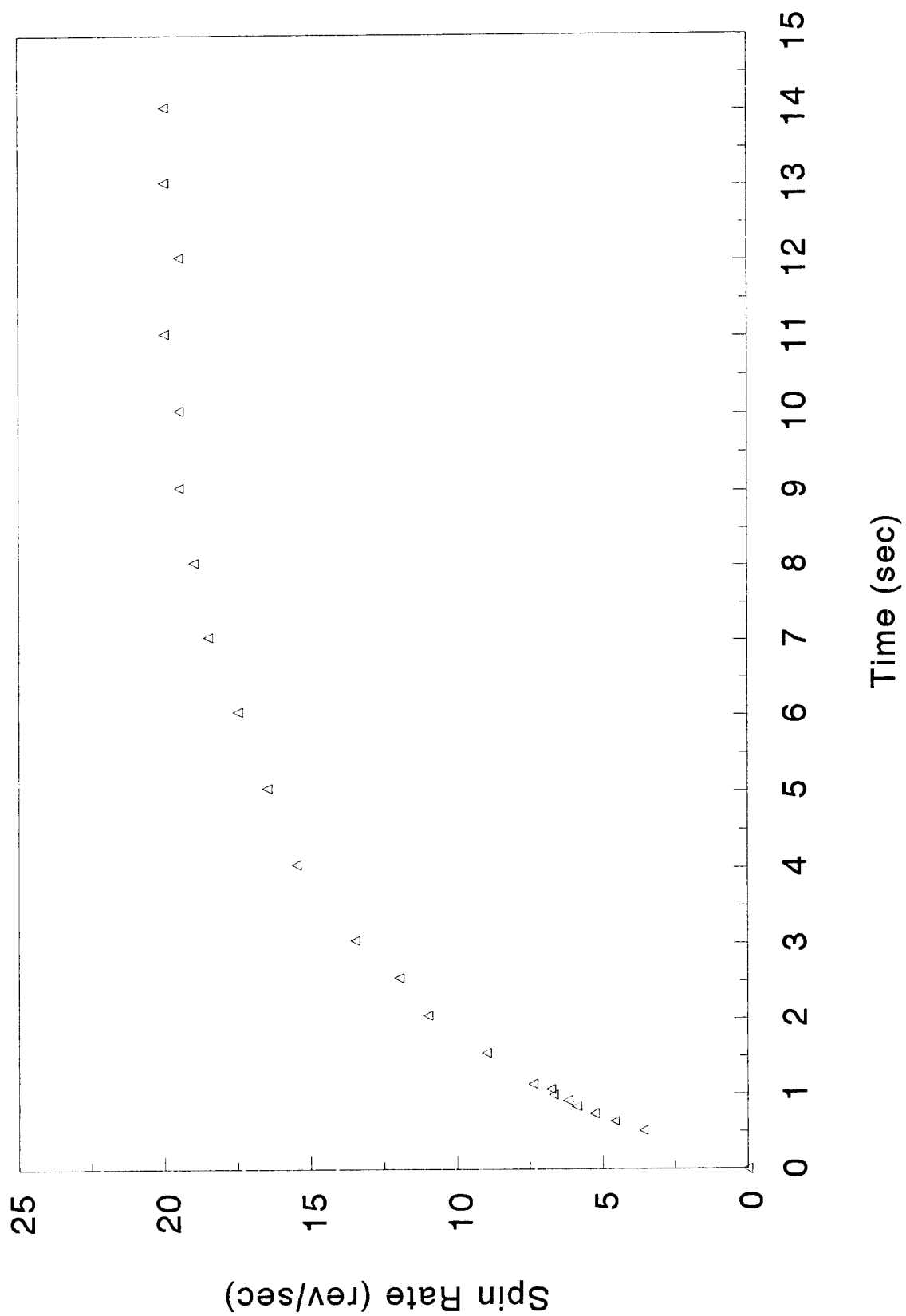
Figure 8
Sample spin rate versus time plot

18
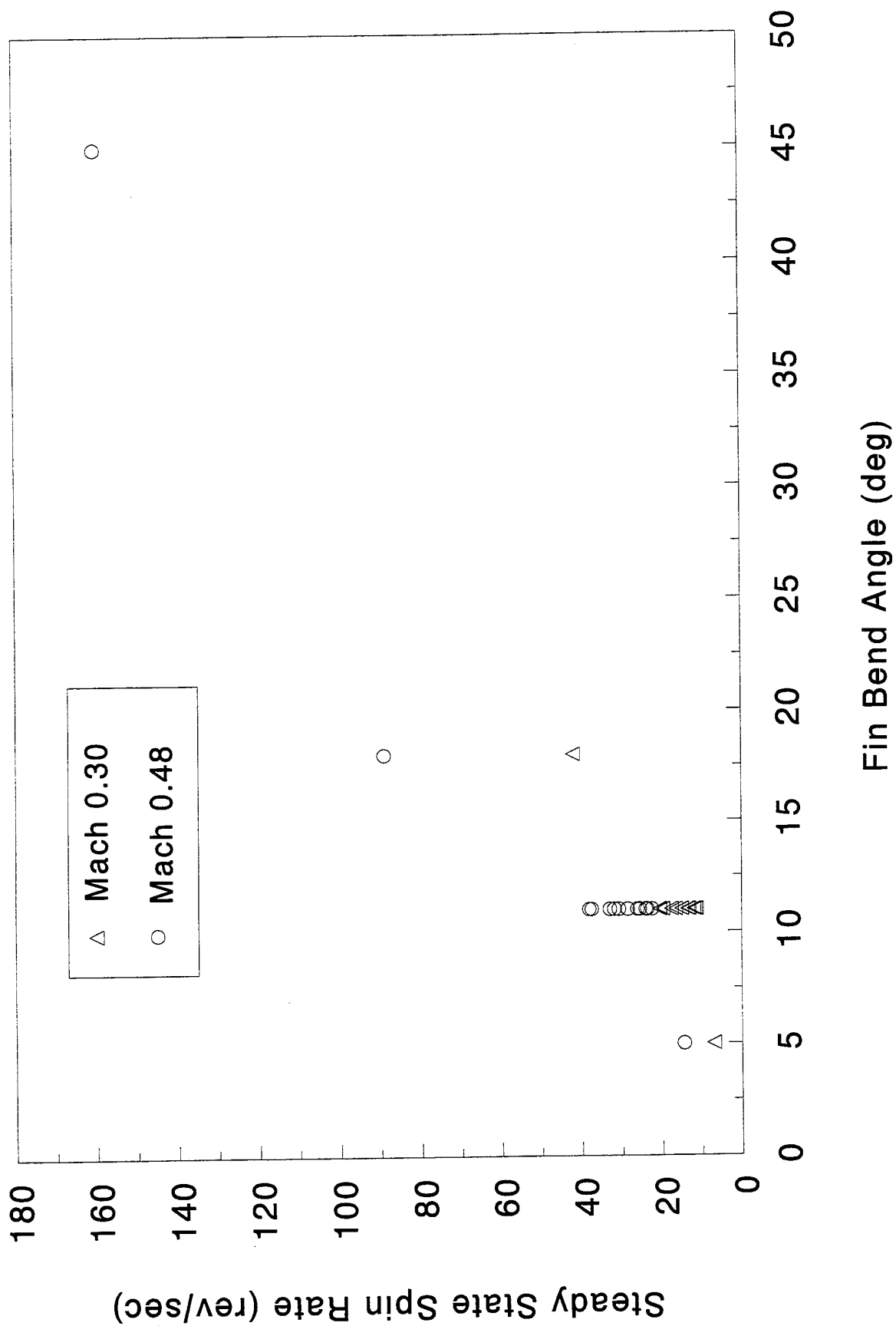
Figure 9
Steady state spin rate versus fin bend angle

Figure 10
Spin rate versus time for uncanted fins (charge 0)

Figure 11
Spin rate versus time for uncanted fins (charge 4)
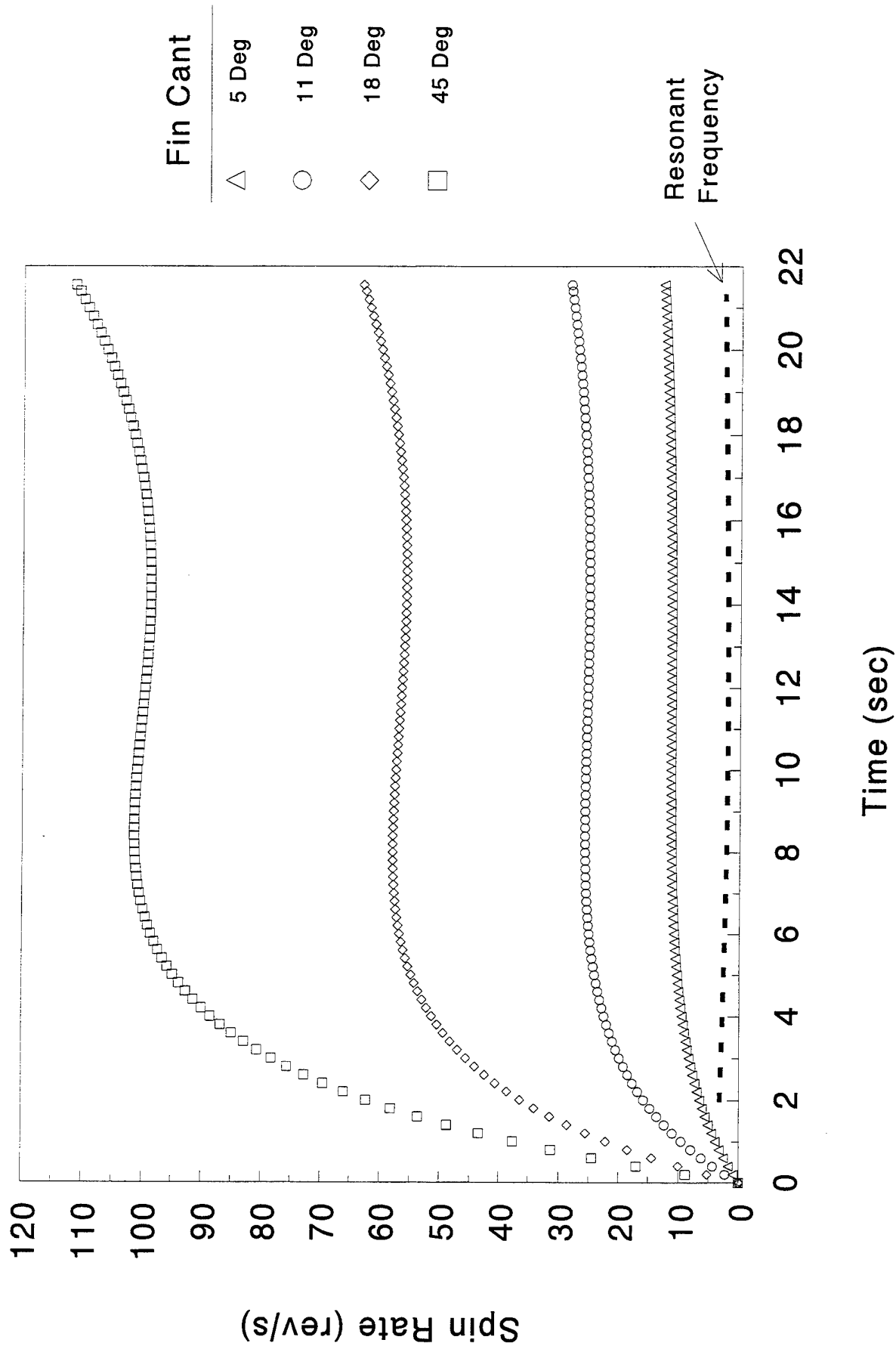
Figure 12
Spin rate versus time for all fin bend angles (charge 4)
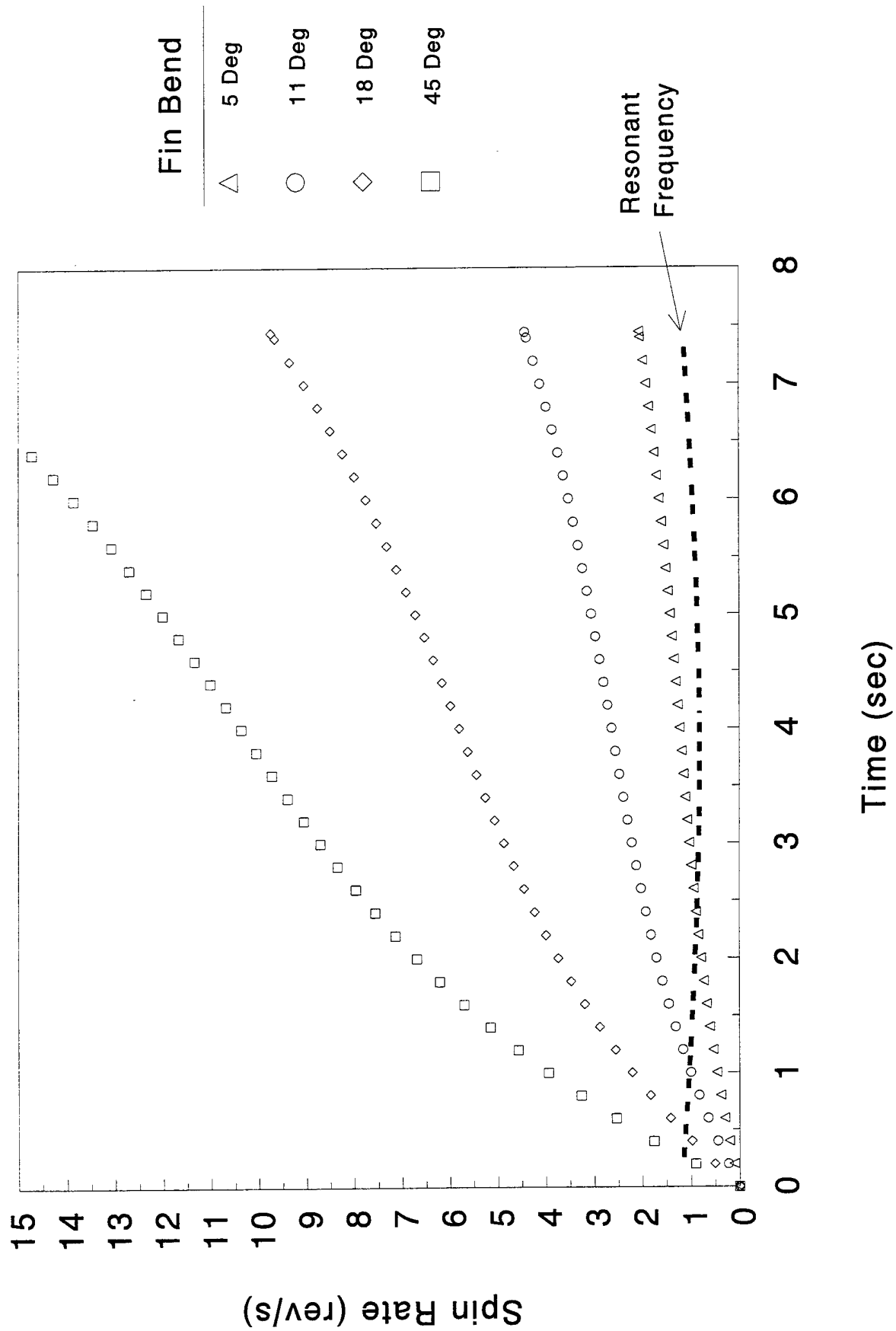
Figure 13
Spin rate versus time for all fin bend angles (charge 0)

23
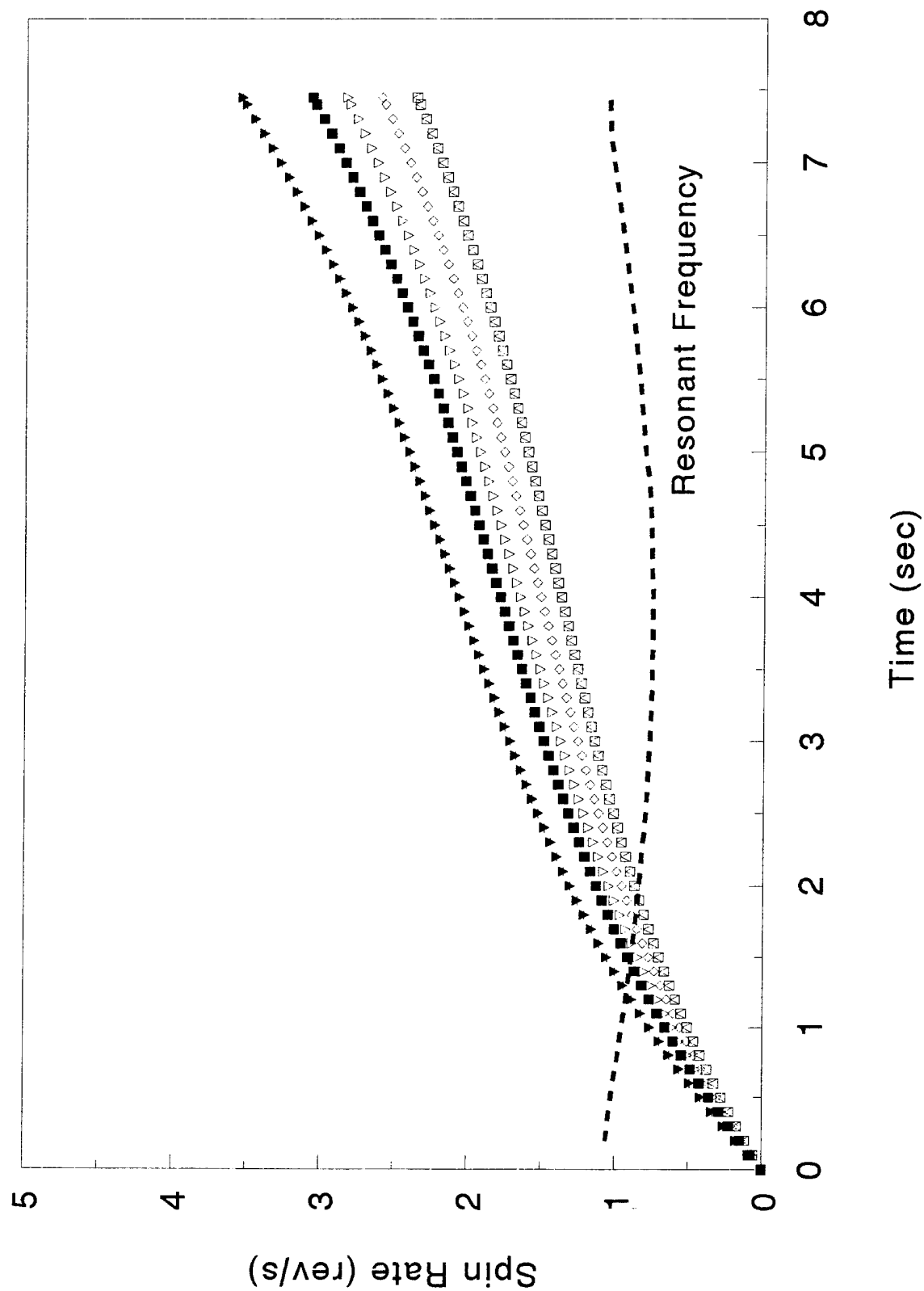
Figure 14
Spin rate versus time for 11 deg bent fins (charge 0)

24
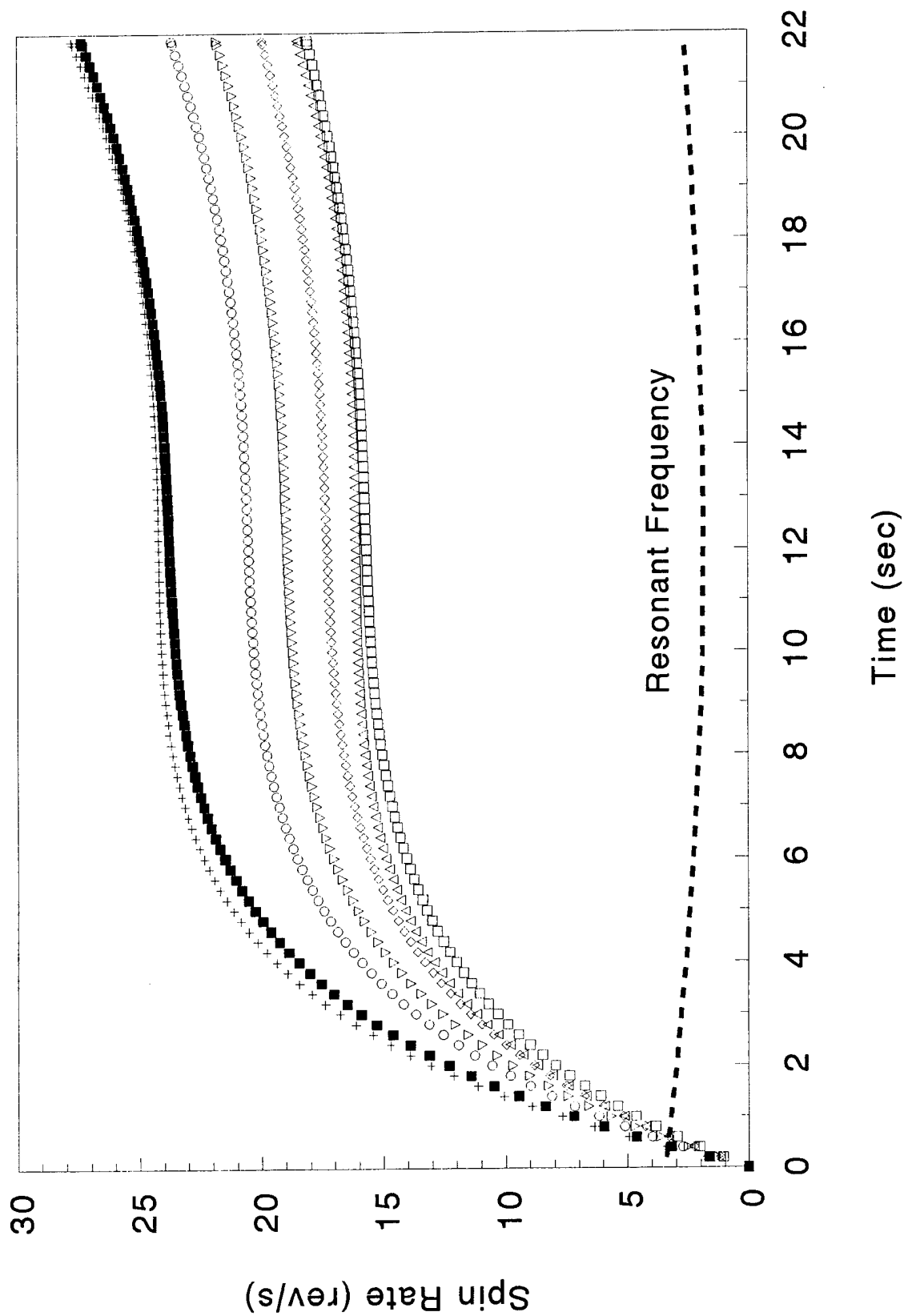
Figure 15
Spin rate versus time for 11 deg bent fins (charge 4)

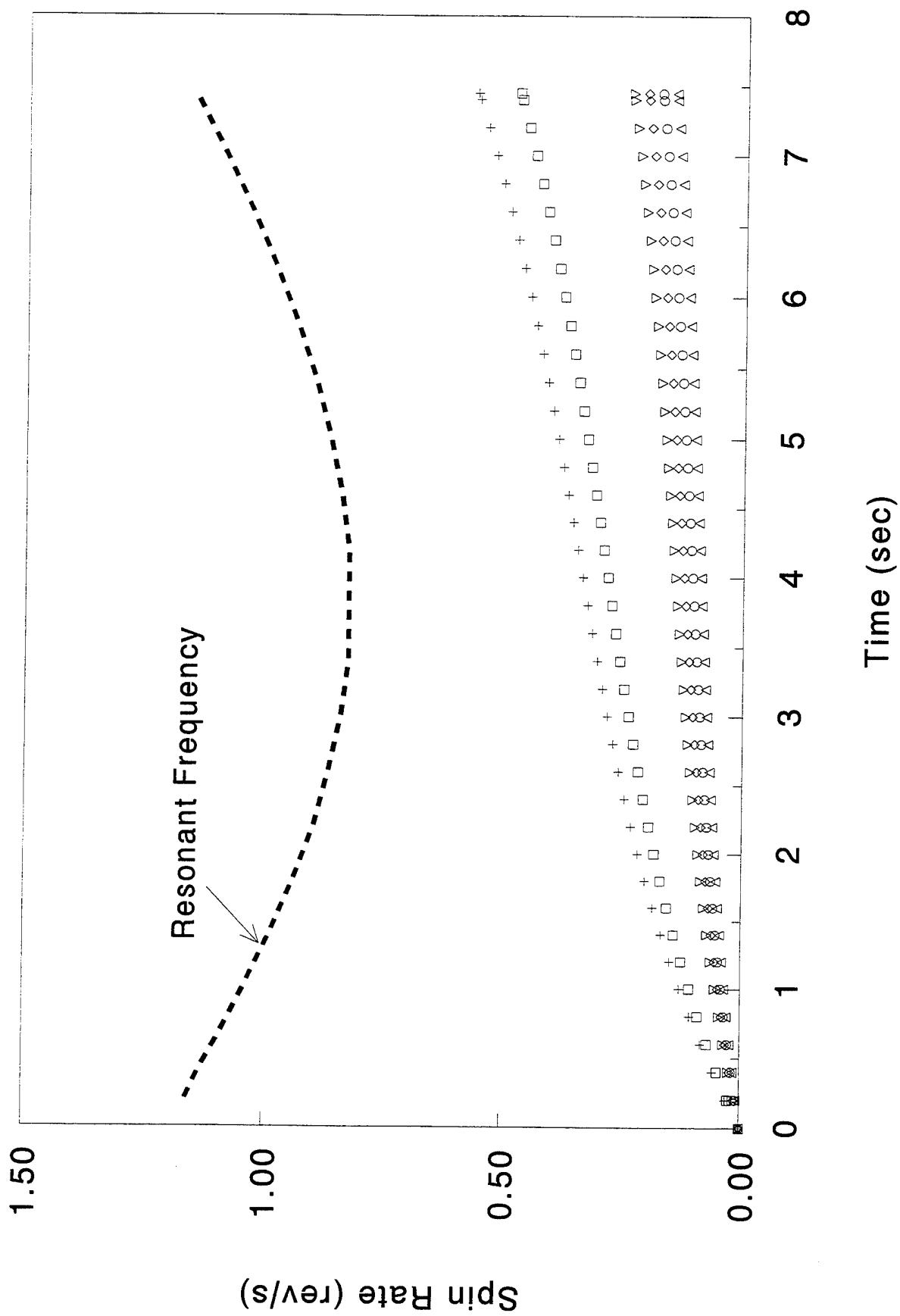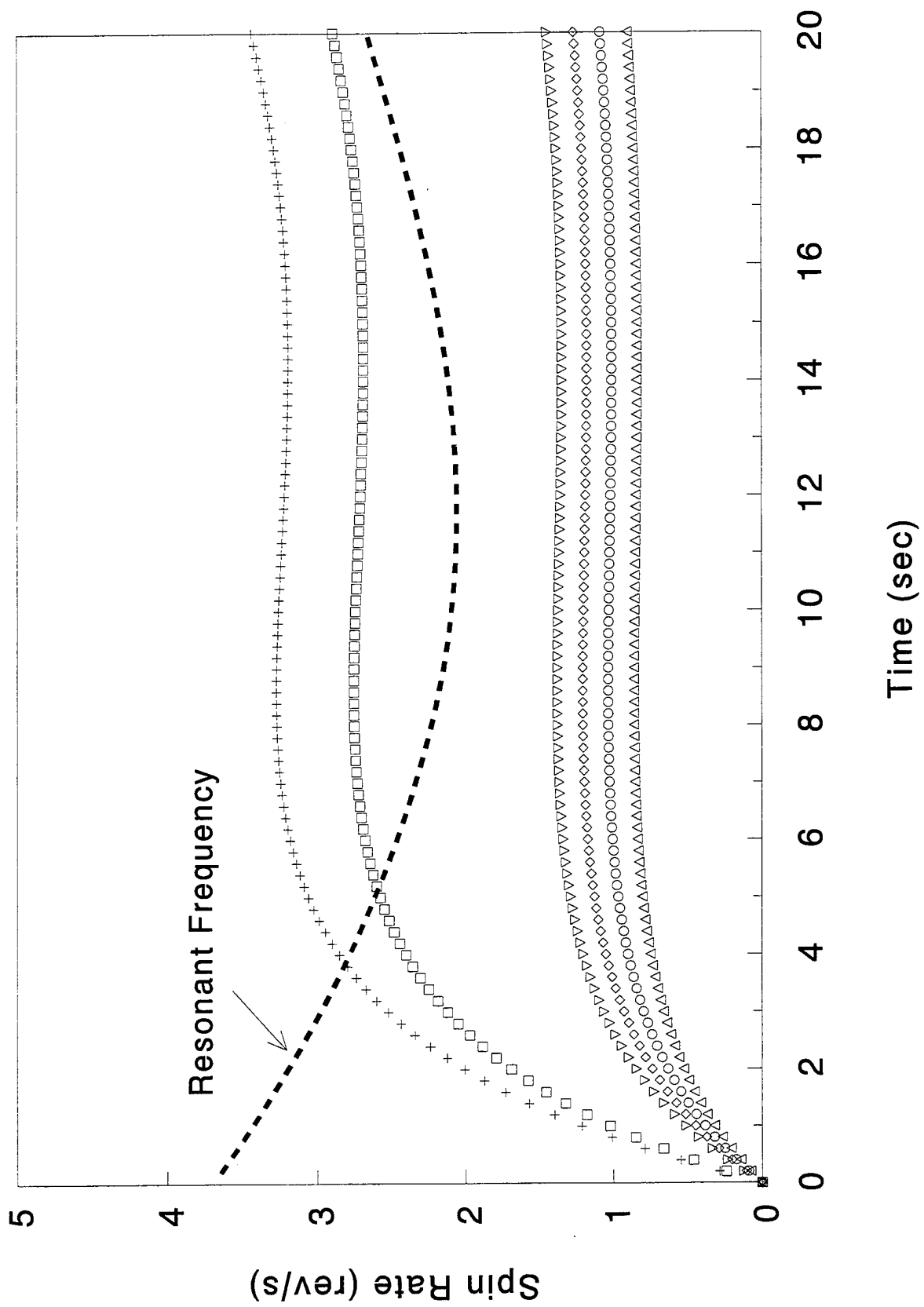## Table 1
Nominal wind tunnel test conditions

	Mach 0.30	Mach 0.48
Total Pressure (psia)	14.35	14.35
Total Temperature (°F)	59.	59.
Dynamic Pressure (psi)	0.81	1.95
Static Pressure (psi)	13.45	12.25
Reynolds No./foot	2.05×10^6	3.10×10^6
Velocity (feet/sec)	330.	530.

Table 2
Wind tunnel test data

| | P_{ss} (rev/s) | | P_o (rev/s2) | |
Configuration	Mach 0.30	Mach 0.48	Mach 0.30	Mach 0.48
5	7.1	15.	-	-
11	20.	38.	7.4	18.
18	42.	90.	16.	50.
45	-	160.	-	77.

Table 3
Aerodynamic roll coefficients

| | C_{l_o} | | C_{l_p} | |
Configuration	Mach 0.30	Mach 0.48	Mach 0.30	Mach 0.48
11	0.017	0.014	-0.36	-0.29
18	0.038	0.040	-0.36	-0.35
45	-	0.059	-	-0.30

Table 4
Roll moment coefficients for a fixed roll damping moment coefficient

Configuration	Mach 0.30	Mach 0.48
5	0.007	0.006
11	0.015	0.015
18	0.033	0.035
45	-	0.059

Table 5
Wind tunnel results for standard M2 fin assemblies

Fin Number	Mach 0.30		Mach 0.48	
	P_{ss}	C_{l_o}	P_{ss}	C_{l_o}
0-1	2.3	0.0022	4.5	0.0019
0-2	-	-	0.4	0.0005
0-3	-	-	0.8	0.0006
0-4	-	-	1.2	0.0008
0-5	-	-	0.5	0.0005
0-6	0.6	0.0012	1.1	0.0007
0-7	-	-	0.8	0.0006
0-8	1.6	0.0018	3.7	0.0016
0-9	---- NOT TESTED ----			
0-10	-	-	1.0	0.0007

Table 6
Results for fins bent to 11 deg

Fin Number	Mach 0.30		Mach 0.48	
	P_{ss}	C_{l_o}	P_{ss}	C_{l_o}
11-0	21.	0.015	38.	0.015
11-1	12.	0.010	24.	0.010
11-2	17.	0.013	31.	0.012
11-3	17.	0.013	32.	0.012
11-4	15.	0.012	29.	0.011
11-5	13.	0.011	26.	0.010
11-6	14.	0.011	26.	0.010
11-7	12.	0.010	24.	0.010
11-8	11.	0.010	23.	0.009
11-9	20.	0.015	37.	0.014
11-10	18.	0.013	33.	0.013

Table 7
Mass and inertial properties for the 60-mm M49A4 projectile

Mass	3.30 lb
Axial Moment of Inertia	1.92 lb-in.^{2}
Transverse Moment of Inertia	27.22 lb-in.^{2}
Center of Gravity	6.65 in. from base

Table 8
Measured roll data for configuration 11-0 at Mach 0.30

Angle of Attack (deg)	P_o (rev/s2)	P_{ss} (rev/s)
-4.	7.1	20.
0.	7.3	20.
4.	6.8	20.
8.	7.2	18.
12.	7.4	20.
16.	7.8	22.
20.	5.8	25

Table 9
Aerodynamic coefficients for configuration 11-0 at Mach 0.30

Angle of Attack (deg)	C_{l_o}	C_{l_p}
-4.	0.016	-0.33
0.	0.016	-0.35
4.	0.016	-0.34
8.	0.016	-0.37
12.	0.017	-0.37
16.	0.017	-0.32
20.	0.014	-0.23

REFERENCES

1. Malejko, Gregory, "The Effect of Fuze Windshield Separation on Flight Performance of the 60-mm, HE, M49A4 Projectile With Fuze, PD, M935,", ARAED-TR-93009, ARDEC, Picatinny Arsenal, NJ, August 1993.

2. Falkowski, E.W., "The Effect on Static Stability and Range of the 60mm, HE, M49A2E2, Mortar Projectile Due to Small Physical Changes, ESL-IR-333, Picatinny Arsenal, NJ, June 1967.

3. "Engineering Design Handbook: Design for Control of Projectile Flight Characteristics", AMCP 706-242, U.S. Army Materiel Command, Washington D.C., September 1966.

4. Whyte, Robert H., "Wind Tunnel Testing Facilities at Picatinny Arsenal", Technical Memorandum 1080, Picatinny Arsenal, NJ, January 1963.

5. Whyte, R.H., "Aerodynamic Characteristics of the M374 81mm Mortar Cartridge," Technical Report 3634, Picatinny Arsenal, NJ, October 1968.

6. Fiorellini, Arthur J. and Grau, John, "An Upgraded Version of the Six-Degree-of-Freedom Trajectory Simulation Computer Program TRAJ - December 1992 Release", Aeroballistics and Structures Branch IR-08-92, Picatinny Arsenal, NJ, December 1992.

7. Wong, Roger, private communication, Picatinny Arsenal, NJ, December 1993.

SYMBOLS

C_{l_o} Roll torque coefficient at zero spin $\left(\dfrac{T_{Roll\ Torque}}{qSd \left(\frac{pd}{2V} \right)} \right)$

C_{l_p} Spin damping coefficient $\left(\dfrac{T_{Roll\ Damping}}{qSd \left(\frac{pd}{2V} \right)} \right)$

C_{m_α} Pitching moment coefficient slope (per radian) $\left(\dfrac{Pitching\ Moment\ Slope}{qSd} \right)$

d Reference diameter (2.362 in.)

I_x Projectile axial moment of inertia

I_y Projectile transverse moment of inertia

p Projectile spin rate

$\dot{p}$ Time rate of change of projectile spin rate

p_{ss} Steady state spin rate

q Dynamic pressure $\left(\frac{1}{2} \rho V^2 \right)$

S Reference area $\left(\dfrac{\pi d^2}{4} \right)$

T Torque

T_{BF} Spin fixture bearing friction torque

$T_{Roll\ Daming}$ Projectile aerodynamic roll damping torque

$T_{Roll\ Torque}$ Projectile roll torque at zero spin

V Velocity

ρ Air density

DISTRIBUTION LIST

Commander
Armament Research, Development and Engineering Center
U.S. Army Tank-automotive and Armaments Command
ATTN: AMSTA-AR-IMC
          AMSTA-AR-GCL
          AMSTA-AR-AE, B. Bushey
                        S. Kahn
          AMSTA-AR-AET, W. Ebihara
          AMSTA-AR-AET-A, J. Grau
                        W. Kuhnle
                        A. Fiorellini
                        R. Trohanowsky
                        G. Malejko (10)
          AMSTA-AR-FSA-M, W. Reilly
                        R. Wong
                        J. Fenneck
                        J. Wejsa
Picatinny Arsenal, NJ 07806-5000

Defense Technical Information Center (DTIC)
ATTN: DTIC-OCC (12)
8725 John J. Kingman Road, Ste 0944
Fort Belvoir, VA 22060-6218

Director
U.S. Army Materiel Systems Analysis Activity
ATTN: AMXSY-MP
Aberdeen Proving Ground, MD 21005-5066

Commander
Chemical/Biological Defense Agency
U.S. Army Armament, Munitions and Chemical Command
ATTN: AMSCB-CII, Library
Aberdeen Proving Ground, MD 21010-5423

Director
U.S. Army Edgewood Research, Development and Engineering Center
ATTN: SCBRD-RTB (Aerodynamics Technology Team)
Aberdeen Proving Ground, MD 21010-5423

Director
U.S. Army Research Laboratory
ATTN: AMSRL-OP-CI-B, Technical Library
Aberdeen Proving Ground, MD 21005-5066

Chief
Benet Weapons Laboratory, CCAC
Armament Research, Development and Engineering Center
U.S. Army Armament, Munitions and Chemical Command
ATTN: SMCAR-CCB-TL
Watervliet, NY 12189-5000

Director
U.S. Army TRADOC Analysis Command-WSMR
ATTN: ATRC-WSS-R
White Sands Missile Range, NM 88002

GIDEP Operations Center
P.O. Box 8000
Corona, CA 91718-8000

Officer in Charge
Naval Weapons Station, Seal Beach
Fallbrook Annex
ATTN: Code 513
Fallbrook, CA 92029